International Journal of Advanced Research in Physical Science (IJARPS)
Volume 2, Issue 11, November 2015, PP 1-10
ISSN 2349-7874 (Print) & ISSN 2349-7882 (Online)
www.arcjournals.org

Analysis of Conduction Mechanism in Zn_2FeNO_3 using Impedance Spectroscopy

A. Elmelouky[1], A.Mortadi[1], R. El Moznine[1], El. Chahid[1]

[1] Laboratoire de Physique de La Matière Condensées (LPMC). Université Chouaib Doukkali, Faculté des sciences, El-Jadida, Morocco

R. Lahkale[2],

[2]Laboratoire de Physicochimie des matériaux(LPCM). Université Chouaib Doukkali Faculté des sciences, El-Jadida, Morocco

Abstract: *Zn-Fe layered double hydroxides (LDHs) were prepared by using the co-precipitation method; with NO_3^- interlayer anion with Zn / Fe ratio (R=2). The structural evolution of Zn_2FeNO_3 was characterized by Riveted analysis on powder X-ray diffraction diagrams. Impedance measurements of Zn_2FeNO_3 were investigated in the frequency range [100Hz–1MHz] and in the temperature range 40°C - 140°C. Cole–Cole plots in impedance spectra showed non-Debye relaxation. The temperature dependence of the relaxation time of Zn_2FeNO_3 showed Arrhenius behavior, from which the activation energy was derived. The real part of ac conductivity spectra of these materials obeys Jonscher power law. The nature of variation of the electrical conductivity, and value of activation energy of Zn_2FeNO_3 , suggest that the conduction process appear clearly related to the structural evolution of the interlayer domain.*

Keywords: *Lamellar, Hydroxide, LDH, Anionic clay, Protonic conduction, Impedance Spectroscopy, X-ray diffraction.*

1. INTRODUCTION

Layered double hydroxides (LDHs), also called anionic (anion-exchanging) clays and hydrotalcite-like compounds Allmann 1970[1] are layered compounds that are based in brucite, Mg (OH). They have a stacking of positively charged octahedral sheets with:

$$\left[M^{II}_{1-x}M^{III}_{x}(HO)_2\right]^{x+}$$

The compositions M^{II} and M^{III} are divalent and trivalent metal ions (Zn, Fe), respectively. The net positive charge, due to substitution of trivalent by divalent metal ions, is balanced by an equal negative charge of Interlayer solvated anions:

$$\left[X^{m-}_{x/m}, \text{x.H}_2O\right]^{x-}, \quad \text{with } X = NO_3^-$$

The hydrated anions in the interlayer spaces can be replaced with almost any desired anion, organic or inorganic, by utilizing simple ion exchange methods.

These compounds showed clearly the M $(OH)_2$ brucite-like main layers, the anionic interlayer domains containing Nitrate ions and water molecules.

In previous works [2–4], the conductivity of LDHs based on different M^{II}-M^{III} pairs, various interlamellar anions and hydration amounts nH_2O were studied; the mainly protonic conduction process was demonstrated by impedantiometric (HP) measurements in an electrochemical gas cell. However, no study has been performed in relation to the structural evolution of the matrix Zn_2FeNO_3.

For use these new materials in a certain molecular electronic device; it is desirable to study their dynamic properties through the dielectric measurement. Dielectric measurements are important technique for studying the dynamic (capacitance, conductivity, and time relaxation and activation energy).

Impedance spectroscopy [4] was used to investigate evolution of ionic conductivity; in a family of Lamellar Double Hydroxides (LDH) with a general formula:

$[Zn_{1-x}Fe_x(OH)_2]^{x+}[NO_3.nH_2O]^{x-}$ In a short notation: $(Zn_{1-x}Fe_x\ (OH)_2X_x.nH_2O)$.

Zn_2FeNO_3 is characterized by high charge density of sheets, modulated via the M^{II}/M^{III} ratio.

Zn_RFeNO_3 [5] were obtained with a broad range of divalent and trivalent metal contents, defined by $x=M^{II} / M^{III} + M^{II}$ with $x_{feuillet}= 0, 33$. In this composition, they display a clear evolution of lattice and structural parameters, but the rhombohedral stacking sequence of the layers is preserved. The positive charge density of these layers is directly proportional to $x_{feuillet}$.

The aim of the present work was to prepare Zn-Fe-LDHs of Zn/Fe ratios (R= 2), NO_3^- in the interlayer space. The exchange ability of interlayer anions depends both on their formal charge (monovalent anions) and on their intrinsic nature (Nitrogen N is strongly held).

This matrix has been characterized using X-ray diffraction XRD, FTIR and ICP techniques. Impedance measurements were also used to analysis of the conduction mechanism in this matrix.

2. EXPERIMENTAL

The Zn_2FeNO_3 matrix was synthesized separately by the constant pH cooprécipitation method. Salts of $ZnCl_2$ ($AlCl_3$ 6H2O), (Fe (NO_3) 3, $9H_2O$) such that the molar ratio Zn^{2+} / Fe^{3+} = 2 for the Zn_2FeNO_3 matrix. Once prepared and dissolved salts in decarbonated water, addition of their solution to a solution of freshly prepared NaOH in decarbonated water should be done under nitrogen dropwise while maintaining the pH at 8. After pouring the entire solution of salts, the resulting colloidal mixture is stirred for 24 hours, well washed several times with decarbonated water, then dried 60 ° C for 48 h and ground into fine for analysis.

2.1. X-Ray Diffraction

The X-ray diffraction patterns were carried out on **D2- PHASER** of **BRUKER-AXS diffractometer** which used K α_1 (1.54056 Å) and K α_2 (1.54439 Å). Generator used at 30 kV and 10 mA. Computation time 15 and 70° (2θ) by step of 0.0101° (0. 2s by step). Program duration is 18mn 06 s.

2.2. Induced Coupled plasma (Icp) Measurements

The metallic ratio what were performed using ICP measurements. A plasma or gas consisting of ions, electrons and neutral particles, is formed from Argon gas, which is then utilized to atomize and ionize the elements in the sample matrix. These resulting ions are then passed through a series of apertures into a high vacuum mass analyzer where the isotopes of the elements are identified by their mass-to-charge ratio The intensity of a specific peak in the mass spectrum is proportional to the amount of the elemental isotope from the original sample, this technique of choice in many analytical for providing the accurate and precise measurements.

Table1. *Elemental Chemical Analysis Data Metals ratio, (%) weight of Fe and Zn in Zn_2FeNO_3*

Matrix	(%) Zn	(%) Fe	R_{exp}	R_{th}
Zn_2FeNO_3	34.5	7.3	1.95	2

3. IMPEDANCE SPECTRSCOPY MEASUREMENT

The impedance measurements were carried out with a 4192 A LF Impedance Analyzer (Hewlett Packard) between 100 Hz and 1 MHz a source of 1V was applied to the electroded pellet samples. The temperature variation was performed using a hot stage with a temperature stability of ± 0.1 K. Silver electrodes were deposited on two circular faces of the sample to get the capacitor shaped sample.

The diameter and the thickness of the sample were 13 mm and 1 mm, respectively. Curve fitting of dielectric spectra with complex empirical functions was carried out using commercial Zview software (version 2.2).

4. RESULTS AND DISCUSSION

4.1. Structural Study

Previous structural results [6–8] were used as a starting point. The rhombohedral symmetry (R-3m space group) is described in its hexagonal setting. The lattice parameter corresponds to the mean distance between two metallic cations in the brucitic layers, and the c lattice parameter to three times

the basal spacing of these layers.

The structural parameters were obtained by the Rietveld method [9] with the Fullprof program [10].Both metallic cations are statistically distributed in **3a** positions of the space group, hydroxyl groups are in (6c), and the interlayer species chloride and oxygen atoms of water molecules are also statistically distributed on the high multiplicity 18(g) position with low (1/6) occupancy.

Fig. 1 shows the X-ray diffraction pattern of the all composition. From the analysis of the spectra, the materials crystallize in the ***R*-3*m*** space group (Rhombohedral phase) with: $\mathbf{c/3 = d_{003} = 2\times d_{006}}$ and a (intermetallic distance**)** $\mathbf{= 2\times d_{110}}$**.**

The cell parameters of the four samples are included in table 2. The c parameter (which represents the thickness of three layers plus the interlayer space between them) was calculated from the average of (00l) reflections. The c parameter decreases as the M^{II}/M^{III} ratio decreases, what has been assigned [11] to stronger interactions between the layers and the interlayer anions.

The structural study gives, notably, access to the evolution with x of the lattice parameters and interatomic distances. The evolution of the lattice parameter **a** is quite linear with x according to equation [12]:

$$a = \sqrt{2}((1-x_{feuillet}).r_{M^{II}} + x_{feuillet}.r_{M^{III}})$$

And is attributed to the corresponding evolution of the mean ionic radius of metallic cations, respectively, 0.74 and 0.64 Å for Zn^{2+} and Fe^{3+} the c lattice parameter, which is directly related to the interlayer distance display, also decreases values when $x_{feuillet}$ increases. This behavior was previously reported [11] and attributed to the increase of charge density on the brucitic layers, leading to stronger interactions with the interlayer anions, although the interlayer domains become more encumbered by the larger chloride anions. We observe in [12] a clear non-linear evolution of c, with a faster decrease at the lowest values of $x_{feuillet}$ [13].

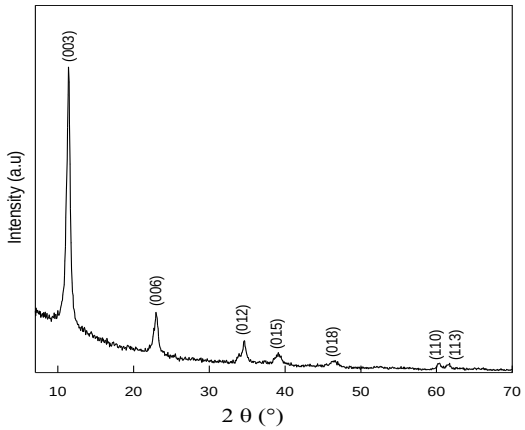

Figure1. *X-ray diffractograms of Zn_2FeNO_3*

Table2. *Values of the lattice parameters **c**, **a** and d_{inter} for Zn_2FeNO_3.*

Matrix	C(A°)	a(A°)	d_{inter}(A°)
Zn_2FeNO_3	23.29	3.09	7.76

4.2. Induced Coupled Plasma (Icp)

The chemical compositions of the constituent LDH are included in Table 1, which shows that the [Zn^{2+} /Fe^{3+}] ratio in the solids is close to that in the starting solutions. The formula in the table considers that chloride is the only compensating anion and does not take into account the possible presence of carbonate impurities in the interlayer space, even for $NO3^-$.

The results of elemental analyses led to an average composition for the solid material which corresponds to the chemical formula: ($Zn_{1.95}$ Fe $(OH)_{5.9}$)(NO_3, 3.07 H_2O) for ratio R=2,

4.3. Infrared Spectroscopy

The corresponding IR spectrum (Fig. 2) presents profiles that resemble those exhibited by all hydrotalcite-like phases. Typical of this spectrum are the large band at 3454.91 cm^{-1} and the band at

1636.32 cm^{-1} which correspond to the valence vibration of hydroxyl groups, υ(OH), as well as the bending vibration of water, $\delta(H_2O)$, respectively. The bands observed in the low-frequency region of the spectrum correspond to the lattice vibration modes and can be attributed to M–O (619.68 cm^{-1}) and O–M–O (426.89 cm^{-1}) vibrations [14]. The most prominent features for NO_3 is the intense sharp peak at 1386 cm^{-1} [15].

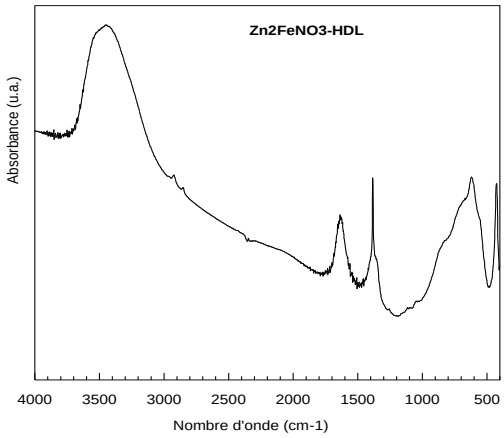

Figure2. *Infrared of Zn_2FeNO_3*

Fig. 3(a) and Fig. 3(b) shows the evolution of the imaginary part Z**"** as a function of the real Z**'** in the frequency range 100Hz–1MHz and at different temperature for Zn_2FeNO_3. Show the similar behavior. When temperature increases the semi-circles become smaller, providing the shift towards lower |Z|. This indicated a reduction of the resistance of the sample. The semi-circles are not perfect but skewed (inclined) with their centers depressed below the real Z'-axis by an angle (a-1) ×p/2, where 0<a<1 [16], that indicates the presence of non Debye type relaxation phenomena caused by a distribution of relaxation time of bulk.

The complex impedance plane plots (Z″ vs. Z') are commonly used to separate the bulk material and the electrode surface polarization phenomena [17, 18, 19–21, 20, 23, 24]. A common feature of samples with dc conductivity is a discontinuity at electrode/sample interface, which has different polarization properties with the bulk material.

In the complex impedance plane plot (Z″ vs. Z') of the MMT clay colloidal suspension in PVP-EG blend [25]; all plots have two separate arcs, which are corresponding to the bulk material effect (the upper frequency arc) and the electrode surface polarization (the lower frequency arc) [17, 18, 19–21, 24, 25]. The frequency values correspond to Z″ minimum value in the plots separates the bulk material and electrode polarization phenomena.

In complex impedance plots; the diameter of arc gives the value of bulk resistance Rb of the sample and hence the σdc values [17]. It is observed that the R_b of these sample decreases with the increase of temperature; and hence the σdc values increases.

The existence of depressed semi-circles in impedance spectra can be explained by a number of phenomena, depending on the nature of the investigated system. In general, the impedance data can be represented as an equivalent circuit, which consists of two parallel of resistance (R)b and constant phase element (CPE)b in series. This is the one of the most common interpretation of phenomena for polycrystalline having a contribution of bulk grain, grain boundary and electrodes [18]. In our measurements; the lowest frequency value (100 Hz) imposed by the instrument HP; the only one arc observed can be attributed to the only bulk contribution of the sample. Therefore; the equivalent electrical circuit was reduced the only one parallel resistance (Rb) and constant phase element (CPE)b to represent the only bulk contribution[19].

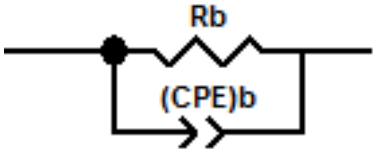

Equivalent electrical circuit of bulk in Zn_2FeNO_3

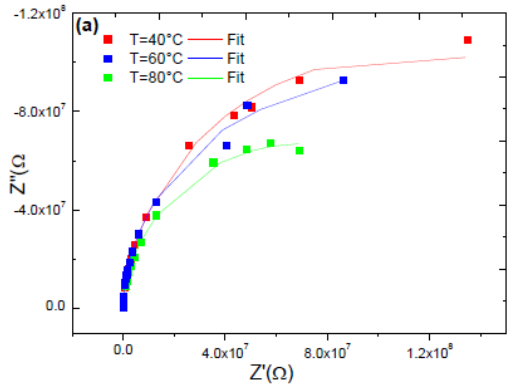

Figure3a. *Complex plane plots (Z'' v.s Z') of Zn_2FeNO_3 For temperatures 40°C, 60°C and 80°C.*

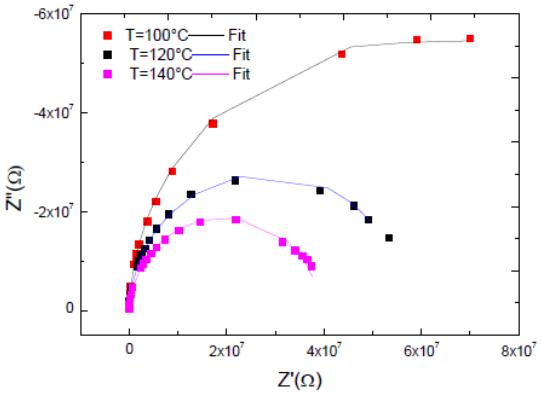

Figure3b. *Complex plane plots (Z'' v.s Z') of Zn2FeNO3 For temperatures 100°C, 120°C and 140°C.*

The value of the Rb was obtained from the intercept of semicircle on the Z' axis and the C (bulk) were calculated using the relation [28, 29]:

$$\omega_{\max} = \tau^{-1} = (RT)^{\frac{-1}{p}} \qquad (0)$$

The relaxation time (τ bulk) was obtained from complex impedance at all temperatures using equation (0). The variation of the bulk resistance R (bulk) and the bulk capacitance C (bulk) with the all temperatures are shown in Fig.4. This indicates that the decrease of the bulk resistance of the sample with an increase of temperature. The values of bulk resistance, Rb, for the single semicircle together with electrode dimensions, were used to determine the bulk electrical conductivity σdc from the equation σ_{dc}=e / (R_b*S), where e is the thickness, and S is the cross section area of the tablet.

The temperature dependence of the bulk DC electrical conductivity σ_{DC} for a representative Zn_2FeNO_3

Sample is shown in Fig.4. This figure shows an increase in the electrical conductivity with increasing temperature. Also, the figure 5 depicts two slopes at the studied temperatures [26] whit activation energies $\Delta E_{ac(dc)}$ equal to 1.20 eV and 4.04 eV in the low and high temperature regions respectively.

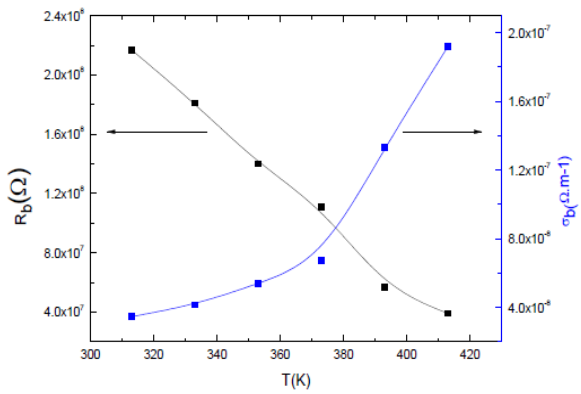

Figure4. *Variation of the bulk resistance R_b and conductivity with all Temperatures.*

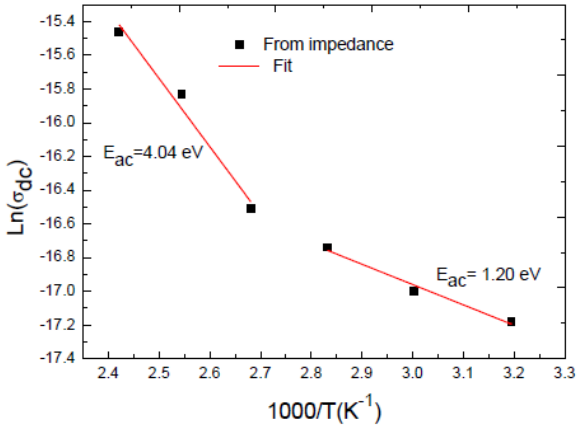

Figure5. *Temperature dependence of σdc for bulk Zn2FeNO3*

4.4. Frequency Dependent Conductivity

The study of frequency dependent conductivity is a well-established method for characterizing the hopping dynamics of the charge carrier. Fig.6 shows typical frequency dependence of AC conductivity at some constant temperature. The behavior of AC conductivity of Zn_2FeNO_3sample exhibits two regions in the studied range of frequency. The total conductivity σ_T of the sample can be described by Jonscher power law [27].

$$\sigma_T(\omega) = \sigma_{dc} + A.\omega^S \qquad (1)$$

Where $\sigma_T(\omega)$ is total conductivity σdc is related to direct conduction and $(A.\omega^s)$ is related to relaxation or polarization conductivity where A is a pre-factor that depends on the temperature and composition and s is the frequency exponent. Both A and s are two temperature dependente parameters. In general, the variation of s, which determined from the linear slope of $Ln(\sigma_{AC}(\omega,T))$ versus in with the temperature is related to the conduction mechanism.

The impedance of constant phase element $(CPE)_b$ can be described as [26]:

$$Z^*_{CPE}(\omega) = \frac{1}{T(j\omega)^p} \qquad (2)$$

Where ω is the angular frequency, T and p are constants and 0 < p < 1. The CPE describes an ideal capacitors with C=T for p=1 and an ideal resistor with R=1/T for p=0. The, p can be used to represent the degree of perfection of the capacitor and represents a measure of arc distortion below the real impedance axis. The parameter p is related with the depression angle as follow:

$$\alpha_d = (1-p)\times\frac{\pi}{2}$$

The complex impedance (Z*) of such circuit (CPE_b//R_b) is as follow

$$Z^*(\omega) = \frac{R}{1+RT(j\omega)^p} \qquad (3)$$

The equation (3) can be written as.

Where: $\tau^p = RT$

$$Z^*(\omega) = \frac{R}{1+(j\omega\tau)^p} \qquad (4)$$

It is important to see that the shape of the equation (3) in impedance complex $Z^*(\omega)$ is similar to the Cole-Cole relaxation in the complex permittivity $\varepsilon^*(\omega)$; except the R at high frequency. Such relaxation is commonly used to analysis the behavior of Ionics conductors [28-29].

In our case; this latter value is close to 0. Therefore the series resistance was not added in the circuit.

The maximum in the imaginary part Z'' (ω) occurs at

$$\omega_{max} = \tau^{-1} = ((RT)^{\frac{-1}{p}}$$

The curve fit of the experimental data was obtained in the whole frequency range using the constant phase element $(CPE)_b$ and resistor R, as shown in Figure 3(a) and Fig. 3 (b).

The resistance R, and the parameters p and T of the $(CPE)_b$ were obtained for each temperature. The values of p are found to lie close to unity (between 0.96 and 0.98). The constant time (τ) of relaxation were then obtained using the relationship given by equation (4). The dc conductivity was derived from the resistance R. Table .3

Give the value of the dc conductivity (σ_{dc}) and the relaxation time (τ) and bulk resistance of Zn_2FeNO_3 at all temperature.

Table3. *Values obtained from fitting circuit of dc conductivity σ_{dc}, bulk resistance R_b and relaxation time at all temperatures.*

T(°C)	$R_b(\Omega)$	$\sigma_{dc}(S.m^{-1})$	τ(s)
40	2.17E+08	3.46E-08	0.0004518
60	1.81E+08	4.15E-08	0.00035226
80	1.40E+08	5.37E-08	0.00023972
100	1.11E+08	6.76E-08	0.00019249
120	5.64E+07	1.33E-07	9.7511E-05
140	3.91E+07	1.92E-07	6.9578E-05

4.5. AC Conductivity Spectra using Circuit Equivalent

Figs. 6. (a), and 6. (b) Show the frequency dependence of σ_{dc} conductivity at several temperatures for Zn_2FeNO_3 and (NO_3^-) respectively. It shows a plateau at low frequencies and dispersion at high frequencies. The plateau region corresponding to dc conductivity is found to extend to higher frequencies when temperature increases. The frequency at which the dispersion takes place, also known as hopping frequency, increases with increasing of the temperature T(K°). This behavior suggests that electrical conductivity occurs via hopping mechanism, which is governed by the Jonscher's power law [28].

$$\sigma_{ac}(\omega) = \sigma_{dc} + A.\omega^n \quad (5)$$

Where, σdc is the direct current conductivity of the sample, ω the angular frequency of measurement. The exponent represents the degree of interaction between mobile ions and with the lattices around them and A is a constant which determines the strength of polarizability.

The frequency dispersion has been attributed to ac conductivity where as the frequency-independent behavior of conductivity in the plateau region corresponds to dc conductivity.

Since the complex conductivity σ_{ac} is related to the complex admittance. This latter can be deduced from the equation (4):

$$Y_b^*(\omega) = \frac{1}{Rb}[1 + (j\omega\tau)^p]$$

$$Y_b^*(\omega) = Y'(\omega) + jY''(\omega) \quad (6)$$

The real and imaginary parts can be written as follow:

$$Y_b'(\omega) = \frac{1}{Rb}\left[1 + (\omega\tau)^p \cos\left(\frac{p\pi}{2}\right)\right] \quad (7)$$

$$Y_b''(\omega) = \frac{1}{Rb}\left[1 + (\omega\tau)^p \sin\left(\frac{p\pi}{2}\right)\right] \quad (8)$$

The real part Y' of function the admittance is related to the ac conductivity $\sigma_{ac}(\omega)$.

$$\sigma_{ac}(\omega) = K * Y'(\omega)$$

Where k is the cell constant:

$$K = \frac{e}{S}$$

The expression ac conductivity:

$$\sigma_{ac}(\omega) = \frac{K}{Rb} + \frac{K}{Rb} * \tau^p \cos\left(\frac{p\pi}{2}\right) * \omega^p \quad (9)$$

The direct current conductivity σ dc can be calculated by the following expression:

$$\sigma_{dc} = \frac{K}{Rb}$$

In the equation (9) the constant A is attributed to the following expression:

$$A = \sigma_{dc}\,(\tau^{p} * \cos\left(\frac{p\pi}{2}\right))$$

$$\sigma_{ac}\,(\omega) = \sigma_{dc} + A * \omega^{p}$$

Therefore the equation (7) becomes the well known Jonscher's power law given in equation (6).

The solid line in the σ_{ac} spectra represent the fit of experimental data to the Jonscher's power law Fig.7.a, b, c the fit values of σ_{dc}, A and n were obtained by Origin non-linear curve fitting software. The values of σ_{dc}, are very close to those obtained from R_b values in the equivalent circuit.

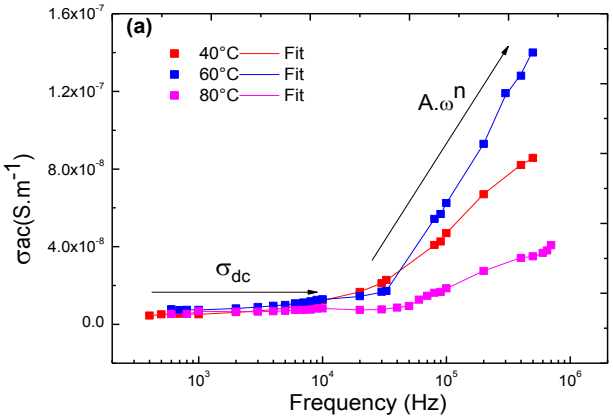

Figure6.a. *Frequency dependence of ac conductivity $\sigma_{ac}(\omega)$ of Zn_2FeNO_3 at 40 ° C ,60 ° C and 80 ° C*

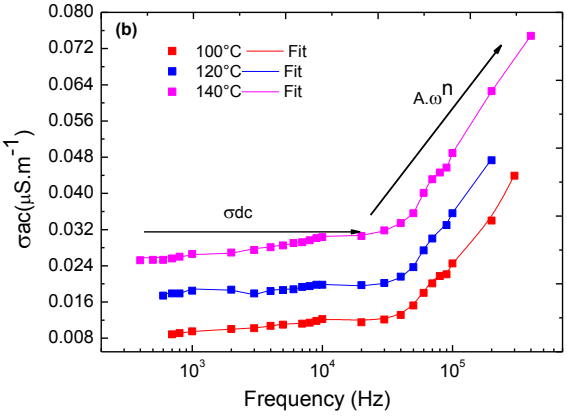

Figure6.b. *Frequency dependence of ac conductivity σac (ω) of Zn2FeNO3 at 100° C, 120 ° C and 140 ° C*

4.6. Conductivity Spectra using Fitting Curve

The behaviour of σ' (ω) spectra were fitted to the Jonscher power law [28] as shown in Fig. a, b, and c:

$$\sigma_{ac}\,(\omega) = \sigma_{dc} + A * \omega^{n} \qquad (5)$$

Where $A * \omega^{n}$ "true ac conductivity" and A is the pre-exponential factor and n is the fractional exponent ranging between 0 and 1 for this material. The solid line in the $\sigma_{ac}\,(\omega)$ spectra denotes the fit of the experimental data to power law expression and the fit values of the dc conductivity s, A and n were obtained using Origin nonlinear curve fitting software and recorded in Table 4. At low frequency, a plateau was observed at in situ temperatures of 100°C, 120°C and 140°C.

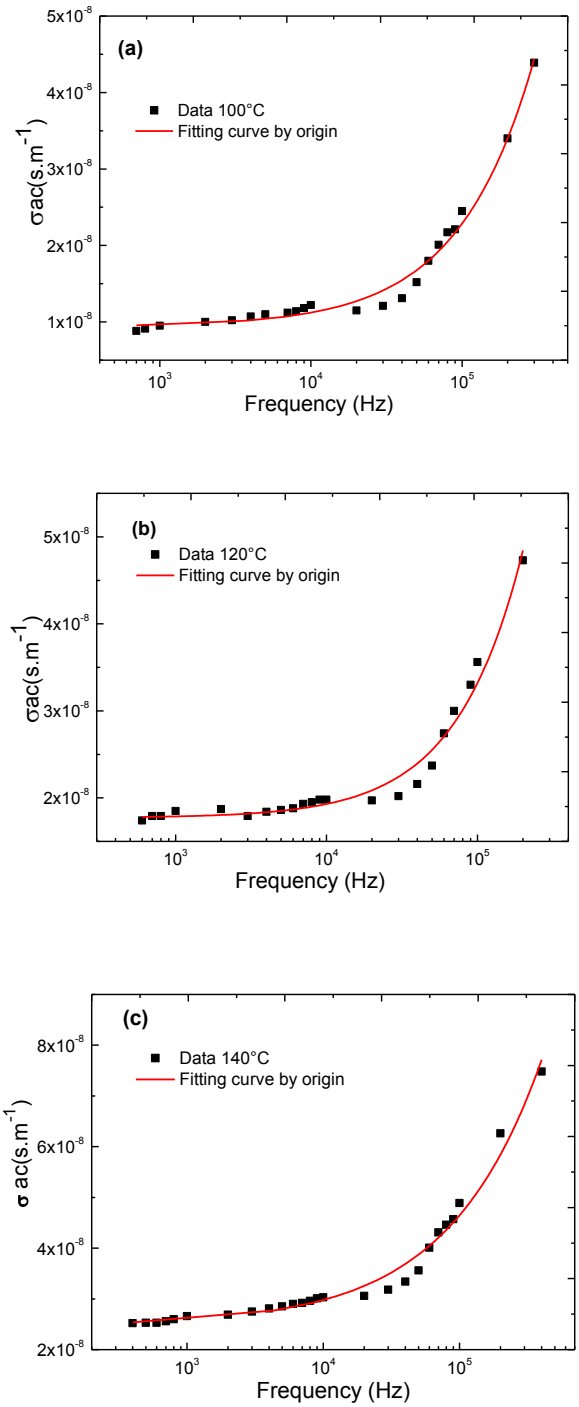

Figures7.*a, b, and c.* *Variation of ac conductivity fitted to the Jonscher power law at true temperatures*

Table4. *Values of dc conductivity, pre-exponential factor A and the fractal exponent n for Zn_2FeNO_3 at true temperatures*

T (°C)	$\sigma_{dc(S/m)}$	A	n	R^2
100°C	9.38E-9	6.11E-13	0.98	0.98
120°C	1.77E-8	1.76E-13	0.98	0.97
140°C	2.47E-8	1.47E-11	0.97	0.98

5. CONCLUSION

Zn_2FeNO_3 layered double hydroxide (Zn_2FeNO_3-LDH) was prepared by the co-precipitation method with a ratio of Zn^{2+}/Fe^{3+} and at a constant pH of 8. Powder XRD patterns showed the characteristic peaks of layered structure of the LDH sample. Infrared spectra of the sample were investigated. Because of the existence of water molecules and anionic NO_3 in the interlayer of the LDH, Chemical

analyses enabled us to confirm the results of the other techniques concerning the intercalation and also to propose an approximate formula for the hybrid material: $(Zn_{1.95}Fe(OH)_{5.9})(NO_3, 3.07\ H_2O)$.

The dielectric spectroscopy of the LDH can be described by an anomalous low frequency dispersion using the second type of Universal Power Law. Novel measurements of activation energy of LDH have been obtained at sex different frequency. The energy value increased the 1.2 eV towards from 4.04 eV. The ionic conductivity (dc) of LDH increased as the in situ temperature increased.

The dielectric response of the LDH is believed to be caused by two charge carriers in interlayer LDH: the protons of the water molecules and the NO_3 interlayer anions, which can be described by the anomalous low frequency dispersion with the second type of Universal Power Law.

REFERENCES

[1] Shigeo Miyata, J.Clays Clay Miner, 23 (1975) 369

[2] E.M. Khaldi, A. de Roy, M. Chaouch, and J.P. Besse., *J. Solid State Chem.126* (1996) 314.

[3] Y. Li, R. Zhang, H. Chen, J. Zhang, R. Suzuki, T. Ohdaira, M. M. Feldstein, Y. C. Jean, *J.Biomacromolecules*, 4(2003) 1856.

[4] V. Ducos, A. de Roy, J.P. Besse, *J. Solid State Ionics* 145(2011) 399.

[5] M. Lakraimi, A. Legrouri, A. Barroug, A. De Roy, J.P. Besse, *J. Mater. Chem.* 10 (2000) 1007.

[6] V.R. Allmann, *J. Chimia* 24 (1970) 99

[7] S. Kim, E-J. Hwang, Y. Jung, M. Han, S-J. Park, *J. Colloid. Surf. A*, 313– 314(2008) 216.

[8] D. K. Pradhan, R. N. P. Choudhary, B. K Samantaray, *J. Express Polym. Lett*, 2 (2008) 630

[9] (a) Z.P. Xu, H.C. Zeng, *J. Phys. Chem*. B 105 (2001) 1743;
(b) Z.P. Xu, H.C. Zeng, *J. Chem. Mater.* 13 (2001) 4564;
(c) F.M. Vichi, O.L. Alves, *J. Mater. Chem*. 7 (1997) 1631.

[10] J. Rodrigues-Carvajal, *J. Mater. Chem.*, 7(1997)801-806

[11] K.M.Parida, Lagnamayee Mohapatr, *J. Chem. Eng* 179 (2012) 131– 139

[12] De la Calle, C., et al., *J. Clays Clay Miner*, 51 (2003)121-132.

[13] M. Oleinikova, M. Munoz, J. Benavente, M. Valiente, *J.* Anal. *Chimi. Acta* 403**,** 91 (2000).

[14] A.Elmelouky, R.Elmoznine, R. Lahkale, R.Sadik, El .Sabbar, EL. Chahid, El. Choukri, Mezzane. *J.Optoelectronics. adv. Mater*.1239-1247(2013)

[15] Sadik. N., Sabbar. E., MOUNTADAR. M, Lakraimi. M., *J. Mater.Environ. Sci*., 3 (2) (2012), 379-390.

[16] R. J. Sengwa, S. Sankhla, *J.Polym. Bull*, 60 (2008) 689

[17] S. Kim, E-J. Hwang, Y. Jung, M. Han, S-J. Park, *J. Colloids Surf; A***,** 313–314 (2008) 216.

[18] D. K. Pradhan, R. N. P. Choudhary, B. K. Samantaray, *J. Express. Polym. Lett* 2, (2008) 630.

[19] R. J. Sengwa, S. Sankhla, *J.Colloid. Polym. Sci*, 285(2007) 1237

[20] R. J. Sengwa, S. Sankhla, *J.Macromol. Sci*, 46 (2007) 717.

[21] R. J. Sengwa, S. Sankhla, *J. Eng. Mater. Sci*, 14 (2007) 317.

[22] P. Pissis, A. Kyritsis, *J. Solid State Ionics*, 97(1997) 105.

[23] R. J. Sengwa, S. Sankhla, J.*Polym* 48, 27 (2007) 37.

[24] A.K. Thakur, D. K. Pradhan, B. K. Samantaray, R. N. P. Choudhary, *J. Power Sources* 159 (2006) 272.

[25] R.J. Sengwa, S. Choudhary, S. Sankhla, *J. Express .Polym. Lett* 11, (2008) 800.

[26] A.A.A. Darwich, E.F.M.EL-Zaidia, M.M.El-Nahass, T.A.Hanafy, A.A. Al-Zubaidi. *J.Alloys compd* 589(2014) 393-398

[27] R. El Moznine, G. Smith, E. Polygalov, P.M. Suherman, J. Brodhead, *J. Phys. D***,** 36 (2003) 330.

[28] K. A. Mauritz, *J.Macromolecules* 22 (1989) 4483.

[29] F. De Guerville, M. El Marssi, I. Luk'yanchuk, L. Lahoche, *J. State Ionics* 8 (1983) 159